IJARSCT
ISSN (Online) 2581-9429
International Journal of Advanced Research in Science, Communication and Technology (IJARSCT)
International Open-Access, Double-Blind, Peer-Reviewed, Refereed, Multidisciplinary Online Journal
Impact Factor: 7.301
Volume 3, Issue 1, June 2023

Hot Electron Energy Loss Rate in Two-Dimensional SiGe Heterostructure

Kasala Suresha
Department of Physics
Government First Grade College, MCC 'B' Block, Davanagere, India

Abstract: *We study the hot electron energy-loss rate (ELR) induced by acoustic phonons and optical phonons, in two-dimensional SiGe quantum wells, including the screening effect and hot-phonon effect. At the low-temperature regime, the ELR is found to be dominated by acoustic phonons and at higher temperature ELR is dominated by optical phonons. The unscreened longitudinal acoustic (LA) phonon due to deformation potential (DP) coupling is dominant over the other screened acoustic phonon contributions. At higher temperatures, there is a crossover from ELR due to LA phonons to ELR due to longitudinal optical (LO) phonons with the cross-over temperature being about Te~40K. The ELR without hot phonon effect in LO phonon scattering is studied. The LA phonon screening effect and hot phonon effect is demonstrated to reduce ELR significantly.*

Keywords: energy loss rate, acoustic phonons, optical phonons, screening effect, hot phonon effect, SiGe, heterostructure

I. INTRODUCTION

Quantum devices are presently an area of intense activity. This is due in part to novel computing opportunities offered by quantum computing and quantum information more generally, and in part by the need to control quantum effects in classical devices. It also underscores a new era of technology, in which it has become possible to control the fundamental quantum degrees of freedom of microscopic objects, even within the confines of a solid-state matrix. Electron spins form an excellent basis for quantum devices, since they may be isolated in quantum dots, artificial or natural, and in principle they can transported to distant locations through quantum channels. The spin variable can be controlled through either electric or magnetic fields [1].

The main challenge for spintronics applications is to manipulate and measure the spins, while simultaneously isolating them from their environment. The degradation of spin information is known as decoherence. In the semiclassical spin field effect transistor (SFET) [2], decoherence leads to diminished functionality of the device, while for spin qubits, decoherence leads to computing errors [3]. Decoherence properties may depend on fundamental materials properties, growth conditions, temperature, or any number of environmental variables. Many variations on these techniques have been developed. Quantum devices provide a challenge for such bulk techniques, since the number of active electrons may be very few. In this case, electrically detected ESR techniques (ED-ESR) play an important role [4]. In the limit of single-electron devices, completely new methods are required, based on single-spin manipulation and readout [5-8].

While many recent advances in quantum devices have occurred in the GaAs materials system, silicon occupies a unique position. On the one hand, the materials environment of silicon has the distinction of having the smallest spin-orbit coupling of any currently practical semiconducting material, due to its high position in the periodic table. Additionally, the predominant isotope of silicon is 28Si, with nuclear spin zero. Modulation-doping, isotopic purification, and clean heterostructures therefore hold the prospect of an environment with very low decoherence. On the other hand, Si quantum wells are clad by SiGe barriers, and therefore intrinsically strained, leading to growth and fabrication challenges. Moreover, as an indirect bandgap material, the conduction band structure of silicon is fundamentally more complicated than that of direct gap materials, leading to decoherence and spin manipulation challenges associated with multiple conduction valleys.

Many factors can effect transport in silicon devices, including variable germanium content in the quantum well and the barriers, use of oxide materials as barriers, proximity of modulation doping layers and their impurity ions, presence of

ISSN 2581-9429 IJARSCT

IJARSCT
ISSN (Online) 2581-9429
International Journal of Advanced Research in Science, Communication and Technology (IJARSCT)
International Open-Access, Double-Blind, Peer-Reviewed, Refereed, Multidisciplinary Online Journal
Impact Factor: 7.301
Volume 3, Issue 1, June 2023

dopants in the quantum well, width of the quantum well, and roughness of the interfaces. It is therefore important to test current theories of scattering in a variety of devices and samples. In the second half of our paper, we present preliminary data obtained from several different samples which have been recently used in the fabrication of quantum devices, including quantum point contacts and few-electron quantum dots. Based on transport data through these devices, we deduce that they are of very high quality. However, the samples are not of the same origin as those used in many recent ESR experiments. We find that while some of the samples show similar ESR behavior as previous experiments, others show differences that cannot be fully explained by existing theories. We conclude that the current understanding of Si structures, especially those of importance for quantum devices, is not yet complete.

II. THEORY

The theoretical purpose of our calculation is a quantum well formed in SiGe/Si heterostructure. In our calculations, we assumed that electron transitions occur within the first size-quantization subband. In the one-phonon process, the momentum and energy conservation requirement prevents the more energetic acoustic phonons from scattering electrons. If and $\boldsymbol{q}$ and $\boldsymbol{q'}$ are the phonon wave vector in the short wavelength regions such that $\boldsymbol{Q} = \boldsymbol{q} + \boldsymbol{q'}$ is quite small so as to lie in the long wavelength region. Further, it will be assumed that the electrons are quasi-2D, with the electron wave function given by

$$\Psi_{\boldsymbol{k}}(\boldsymbol{r}) = \frac{1}{\sqrt{A}} e^{i\boldsymbol{k}*\boldsymbol{r}}\, \Phi(z) \qquad (1)$$

where A is the area in the plane of the layer, $\boldsymbol{k}$ and $\boldsymbol{r}$ are the usual two-dimensional vectors. Here only the first subband is assumed to be occupied.

It is convenient to calculate average energy loss per electron by calculating the energy gained by phonons from the electrons and dividing by the number of electrons (N_e) participate [9]

$$\langle P\rangle = -\frac{1}{N_e}\sum_{\boldsymbol{k},\boldsymbol{q},\boldsymbol{q'}} \hbar\left(w_{\boldsymbol{q}} + w_{\boldsymbol{q'}}\right)\frac{2\pi}{\hbar}\{\left(N_{\boldsymbol{q}}+1\right)\left(N_{\boldsymbol{q'}}+1\right)f(E_{\boldsymbol{k'}})[1-f(E_{\boldsymbol{k}})] \qquad (2)$$

$$- N_{\boldsymbol{q}}N_{\boldsymbol{q'}}f(E_{\boldsymbol{k}})\,[1-f(E_{\boldsymbol{k'}})]\}\; |M(\boldsymbol{q},\boldsymbol{q'})|^2\, \left|F\left(\boldsymbol{q}_{z,}\boldsymbol{q}_{z'}\right)\right|^2 \delta(E_{\boldsymbol{k'}} - E_{\boldsymbol{k}} - \hbar(w_{\boldsymbol{q}} + w_{\boldsymbol{q'}}))$$

with $f(E_{\boldsymbol{k}})$ and $N_{\boldsymbol{q}}$ respectively representing the Fermi distribution with T_e and Bose distribution with T_L. $\left|F\left(\boldsymbol{q}_{z,}\boldsymbol{q}_{z'}\right)\right|^2$ is the overlap integral.

II-A. ELECTRON-ACOUSTIC DEFORMATION POTENTIAL SCATTERING:

Following the subband procedure and assuming the phonon modes to be the same as those of bulk semiconductors, one can calculate the expression for the energy loss rate for screened acoustic deformation potential, piezoelectric scattering for the average electron energy loss rate due to screened acoustic deformation potential scattering can be expressed as

$$\langle P\rangle_{DP} = \frac{E_d^2 m^* k_F}{4N_S\pi^2\rho\hbar}\int_0^\infty\int_0^\infty q^2 S^2(q_\parallel)\, F_1(\boldsymbol{q})\, \gamma(\eta_-,\eta_+)dq_\parallel dq_z \qquad (3)$$

where $F_1(\boldsymbol{q}) = |F(q_z)|^2\left[exp\left\{\frac{\hbar\omega_{\boldsymbol{q}}}{k_B}\left(\frac{1}{T_L}-\frac{1}{T_e}\right)\right\}-1\right]N_{\boldsymbol{q}}$

and $\gamma(\eta_-,\eta_+) = \int_0^\infty \frac{1}{\sqrt{X}} f(X+\eta_-^2)[1+f(X+\eta_+^2-\mu)]dX$

where $f\left(X+\eta_\pm^2\right) = \frac{1}{[exp\{\xi(X+\eta_\pm^2)\}+1]}$

with $\eta_\pm^2 = \left(\frac{q_\parallel}{2k_F} \pm \frac{m^*\omega_{\boldsymbol{q}}}{\hbar k_F q_\parallel}\right)^2$, and $\xi = \frac{E_F}{k_B T_e}$ and $\mu = \frac{E_f}{E_F}$ with $E_f = k_B T_e \ln\left[\exp\left(\frac{E_F}{k_B T_e}\right)-1\right]$, where Fermi energy, $E_F = \left(\frac{\pi\hbar^2 N_S}{m^*}\right)$

The screening function, $S^2(q_\parallel) = \left[1+\frac{q_s}{q_\parallel}H(q_\parallel)\right]^{-2}$ with screening parameter, $q_s = \left(\frac{2m^*e^2}{\varepsilon_s\hbar^2}\right)$.

The screening form factor, $H(q_\parallel) = \frac{b\,(8b^2+9bq_\parallel+3q^2)}{8(b+q_\parallel)^3}$ for heterojunction and

$H(q_\parallel) = \frac{4}{4\pi^2+L^2{q_\parallel}^2}\left[\frac{3}{4}Lq_\parallel + \frac{2\pi^2}{Lq_\parallel} - \frac{8\pi^4(1-e^{-Lq_\parallel})}{L^2{q_\parallel}^2(4\pi^2+L^2{q_\parallel}^2)}\right]$ for Quantum Wells.

IJARSCT
ISSN (Online) 2581-9429
International Journal of Advanced Research in Science, Communication and Technology (IJARSCT)
International Open-Access, Double-Blind, Peer-Reviewed, Refereed, Multidisciplinary Online Journal
Impact Factor: 7.301
Volume 3, Issue 1, June 2023

II-B. ELECTRON-ACOUSTIC PIEZOELECTRIC POTENTIAL SCATTERING:

Similarly, the average electron energy loss rate for screened acoustic piezoelectric scattering

$$\langle P\rangle_{PZ} = \frac{(eh_{14})^2 m^* k_F}{4N_s\pi^2\rho\hbar}\int_0^\infty\int_0^\infty A_i S^2(q_\parallel)\, F_1(\boldsymbol{q})\,\gamma(\eta_-,\eta_+)dq_\parallel dq_z \quad (4)$$

where A_i for longitudinal piezoelectric scattering is given by $A_l = \left(\frac{9q_\parallel{}^4 q_z^2}{2q^6}\right)$ and for transverse piezoelectric scattering $A_t = \left(\frac{8q_\parallel{}^2 q_z^4 + q_\parallel{}^6}{2q^6}\right)$. h_{14} is the piezoelectric coupling constant.

II-C. ELECTRON-LONGITUDINAL OPTICAL PHONON POTENTIAL SCATTERING:

Including the hot-phonon effect, the average energy loss rate due to longitudinal optical (LO) phonon scattering can be expressed as

$$\langle P\rangle_{LO} = \frac{(\hbar w_o)^2 m^* k_F e^2}{N_s\pi^2\hbar^3\varepsilon'}\int_0^\infty\int_0^\infty q^{-2}\, F(w_o, q_z)\,\gamma(\eta_-,\eta_+)\, dq_\parallel dq_z \quad (5)$$

Where $\gamma(\eta_-,\eta_+) = \int_0^\infty \frac{1}{\sqrt{X}}\, f(X+\eta_-^2)[1 - f(X+\eta_+^2)]\, dX$ (6)

with $f(X+\eta_\pm^2) = \left[exp\{\xi(X+\eta_\pm^2-\mu)\}+1\right]^{-1}$; $\eta_\pm^2 = \left(\frac{q_\parallel}{2k_F} \pm \frac{m^* w_q}{\hbar k_F q_\parallel}\right)^2$; $\xi = \frac{E_F}{k_B T_e}$; $\mu = \frac{E_f}{E_F}$

and $F(w_o, q_z) = |F(q_z)|^2 \left[N_q^{HP}\left(exp\left\{-\frac{\hbar w_o}{k_B T_e}\right\}-1\right) + \left(exp\left\{-\frac{\hbar w_o}{k_B T_e}\right\}\right)\right]$ (7)

here N_q^{HP} is the non-equilibrium distribution function of phonons given by

$$N_q^{HP} = \left[\frac{N_q + \tau_p\,\alpha\left(exp\left\{-\frac{\hbar w_o}{k_B T_e}\right\}\right)}{1+\tau_p\,\alpha\left(1 - exp\left\{-\frac{\hbar w_o}{k_B T_e}\right\}\right)}\right] \quad (8)$$

with τ_p be the optical phonon life time and α is given by

$$\alpha = \frac{2m^* k_F e^2(\hbar w_o)}{\hbar^3 L\varepsilon' q_\parallel q^2}\,|F(q_z)|^2\,\gamma(\eta_-,\eta_+) \quad (9)$$

with $\varepsilon' = \left(\frac{1}{\varepsilon_\infty} - \frac{1}{\varepsilon_s}\right)^{-1}$

The total power loss per electron is obtained by adding contribution from LA deformation, piezoelectric and LO phonons (equations 3, 4 and 5).

III. RESULTS AND DISCUSSION

Theoretical calculations of power loss per electron P as a function of electron temperature for acoustic deformation potential, acoustic piezoelectric scattering and longitudinal optical phonon processes have been performed for the SiGe/Si quantum well heterostructure. The material parameters used in calculations characteristic of SiGe are $m^* = 0.92m_0$, V_s =8.433x10^3 m/s, ρ = 2329 kg/m^3, $\hbar w_o$ = 50.0 meV, τ_p= 10.0 ps, ε_∞ = 7.45 and ε_s = 11.7.

Figure 1 shows the contributions to average energy loss rate from acoustic deformation potential, acoustic piezoelectric and longitudinal optical phonon scattering mechanisms. In calculations we used carrier concentration N_s = 1.0x10^{13} m^{-2}, quantum well width L = 50 A^0, lattice temperature T_L = 3.0K deformation potential constant E_d = 12.0 eV and h_{14} = 0.6x10^9 V/m. In the temperature region we considered here indicates that acoustic deformation potential scattering mechanism is dominant mechanism compared to piezoelectric scattering mechanism. The same dominant mechanism was also observed in 2D GaAs, GaN, GaInAs quantum wells [9-11]. In the acoustic deformation potential scattering mechanism, the only adjustable parameter is the deformation potential constant E_d. While calculating energy loss rate for LO phonon scattering, we assumed the optical phonon energy $\hbar w_o$ =50.0 meV, τ_p= 10.0 ps. The only adjustable parameter for LO phonon scattering mechanism is the optical phonon life time τ_p. When the experimental observations are available for this SiGe quantum wells, these theoretical calculations will show good agreement with the observations. In the figure 1, the pink line shows the energy loss rate for piezoelectric scattering, olive line shows for acoustic deformation potential scattering. In both the scattering mechanisms, we used the dynamical screening effect as this screening effect will reduce the ELR significantly [9,10]. It is clear that, the piezoelectric scattering is completely negligible for this SiGe heterostructure. Therefore the dominant scattering mechanism is due to the acoustic deformation potential in the lower temperature range (T_e<50 K). This study has already been published [12]. The dark

ISSN
2581-9429
IJARSCT

IJARSCT

ISSN (Online) 2581-9429

International Journal of Advanced Research in Science, Communication and Technology (IJARSCT)

International Open-Access, Double-Blind, Peer-Reviewed, Refereed, Multidisciplinary Online Journal

Impact Factor: 7.301

Volume 3, Issue 1, June 2023

line shown the contribution of ELR from LO phonon scattering with hot phonon effect and the blue line represents the total contribution of ELR from screened acoustic (DP+PZ) and longitudinal optical (LO) scattering mechanism with hot phonon effect.

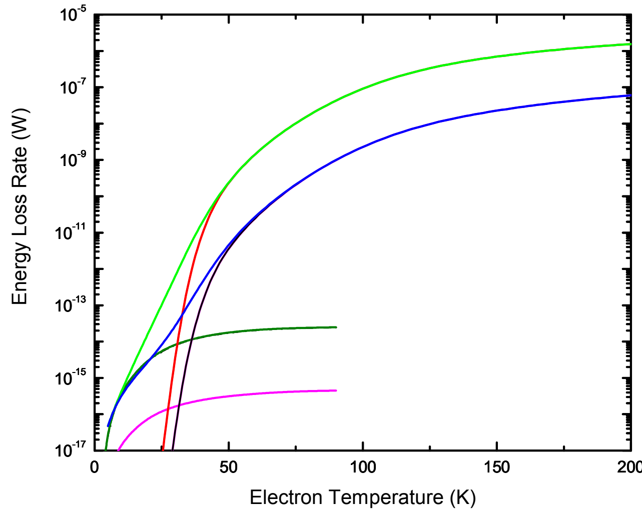

Figure 1: Electron energy loss rate as a function of electron temperature. The blue dashed line represents contribution due to piezoelectric scattering, red dash-dot line for deformation potential scattering and black continuous line for total contribution from both scattering mechanisms.

The red line shown the contribution of ELR from LO phonon scattering without hot phonon effect and the green line represents the total contribution of ELR from screened acoustic (DP+PZ) and longitudinal optical (LO) scattering mechanism without hot phonon effect. We can clearly observe that, the inclusion of hot phonon effect will reduce ELR appreciably.

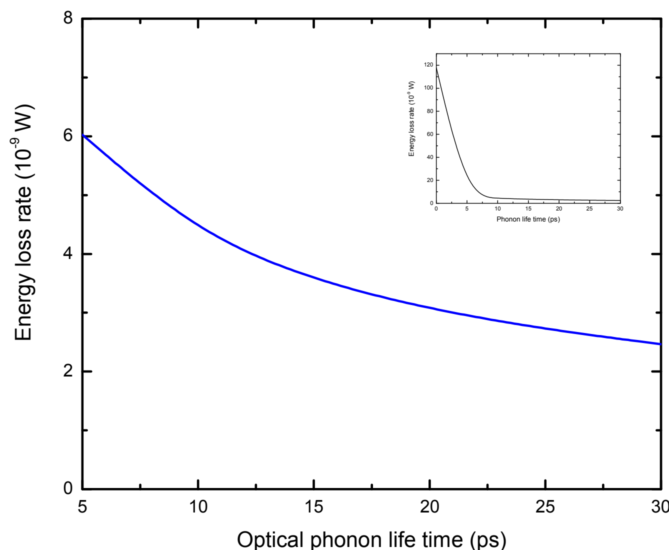

Figure 2: The variation of electron energy loss rate with optical phonon life time.

In our calculations for LO phonon scattering at T_e= 100 K, we assumed optical phonon life time to be 10.0 ps and is the only adjustable parameter to make good agreement with the experimental observations. This type adjustment for optical phonon life time is made in many GaAs, GaAlAs, GaN heterostructures to obtain agreement with observed LER data.

So that, we also tried to study how ELR vary with optical phonon life time which is shown in Figure 2. It is observed cleary that, as the phonon life time increases there is considerable reduction in ELR. The inset of Figure 2 shows the zero phonon life time. If the phonon life time to be zero, it gives the data same as that for ELR without hot phonon effect, indicating the enhancement of ELR by an order of magnitude two.

IV. CONCLUSION

The average energy loss rate in SiGe/Si quantum well through acoustic deformation potential, acoustic piezoelectric and longitudinal optical phonon scattering on the carrier temperature were calculated. The acoustic phonon scattering mechanism is primary scattering mechanism in the lower temperature range. At higher temperature, LO phonon scattering mechanism dominates. In our calculations, we incorporate the hot phonon effect which will reduce the ELR considerably. We also studied the variation of ELR with optical phonon life time indicating the further decline of ELR as the phonon life time increases.

REFERENCES

[1]. I. Zuti´ ˇ c, J. Fabian, S. Das Sarma: Spintronics: Fundamentals and applications, Rev. Mod. Phys. **76**, 323–410 (2004)

[2]. S. Datta, B. Das : Electronic analog of the electro-optic modulator, Appl. Phys. Lett. **56**, 665–667 (1990)

[3]. M.A. Nielsen, I.L. Chuang: Quantum computation and quantum information, (Cambridge University, Cambridge 2000)

[4]. D. Stein, K. von Klitzing, G. Weimann: Electron spin resonance on GaAsAlxGa1−xAs heterostructures, Phys. Rev. Lett. **51**, 130–133 (1983)

[5]. M. Ciorga, A.S. Sachrajda, P. Hawrylak, C. Gould, P. Zawadzki, S. Jullian, Y. Feng, Z. Wasilewski: Addition spectrum of a lateral dot from Coulomb and spin blockade spectroscopy, Phys. Rev. B **61**, R16315–R16318 (2000).

[6]. T. Fujisawa, D.G. Austing, Y. Tokura, Y. Hirayama, S. Tarucha: Allowed and forbidden transitions in artificial hydrogen and helium atoms, Nature (London) **419**, 278–281 (2002)

[7]. J.M. Elzerman, R. Hanson, L.H. Willems van Beveren, B. Witkamp, L.M.K. Vandersypen, L.P. Kouwenhoven: Single-shot read-out of an individual electron spin in a quantum dot, Nature (London) **430**, 431 (2004)

[8]. F.H.L. Koppens, J.A. Folk, J.M. Elzerman, R. Hanson, L.H. Willems van Beveren, I.T. Vink, H.P. Tranitz, W. Wegscheider, L.P. Kouwenhoven, L.M.K. Vandersypen: Control and detection of singlet-triplet mixing in a random nuclear field, Science **309**, 1346–1350 (2005)

[9]. S S Kubakaddi, Kasala Suresha and B G Mulimani, Semicond. Sci. Technol. **17**, 1 (2002)

[10]. S S Kubakaddi, Kasala Suresha and B G Mulimani, Physica E, **18**, 475 (2003)

[11]. Kasala Suresha, J. Critical Rev. **05**, 7 (2018)

[12]. Kasala Suresha, Int. J. Res. Appl. Sci. and Engg. Technol. **11**, 1103 (2023)